JOC The Journal of Organic Chemistry

Article

Kinetic Analysis and Mechanism of the Hydrolytic Degradation of Squaramides and Squaramic Acids

Marta Ximenis, Emilio Bustelo, Andrés G. Algarra, Manel Vega, Carmen Rotger, Manuel G. Basallote, and Antonio Costa

J. Org. Chem., **Just Accepted Manuscript** • DOI: 10.1021/acs.joc.6b02963 • Publication Date (Web): 20 Jan 2017

ACS Publications

The Journal of Organic Chemistry is published by the American Chemical Society. 1155 Sixteenth Street N.W., Washington, DC 20036

Kinetic Analysis and Mechanism of the Hydrolytic Degradation of Squaramides and Squaramic Acids.

Marta Ximenis,[†] Emilio Bustelo,[‡] Andrés G. Algarra,[‡] Manel Vega,[†] Carmen Rotger,[†] Manuel G. Basallote,*[‡] and Antonio Costa.*[†]

† Department of Chemistry, Universitat de les Illes Balears, Palma, 07122, Spain.

‡ Department of Materials Scientist, Metallurgic Engineering and Inorganic Chemistry, Universidad de Cádiz, Puerto Real, 11510, Cádiz, Spain.

E-mail: antoni.costa@uib.es

E-mail: manuel.basallote@uib.es

Tel.: +34 971 173266. Fax: +34 971 173426.

KEYWORDS. Squaramides • Squaramic acids • Hydrolysis • Kinetics• DFT calculations

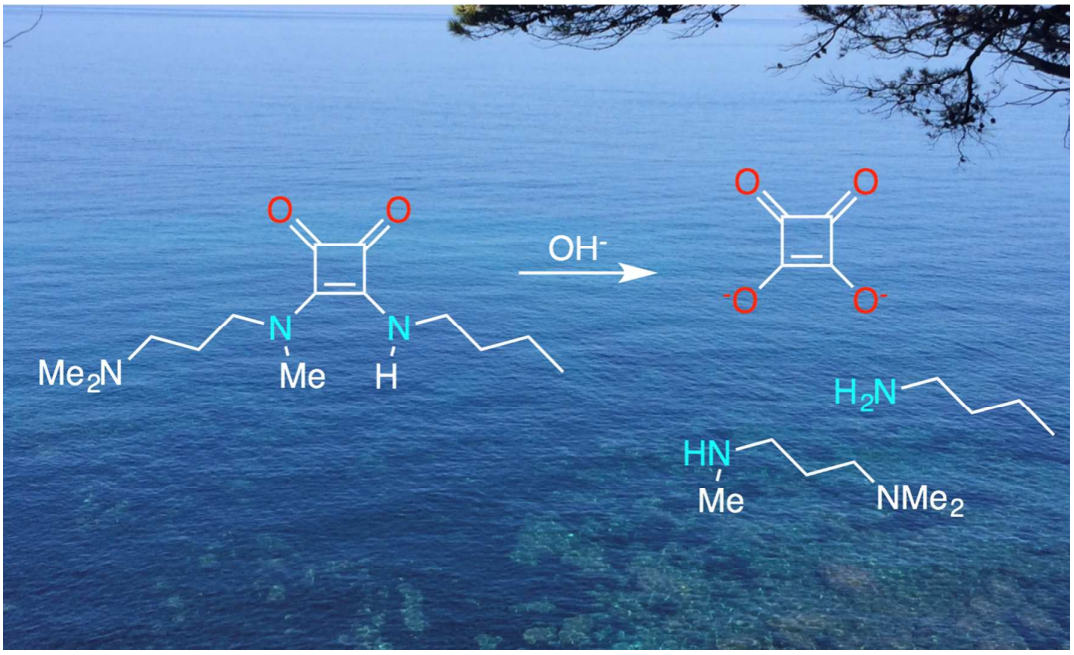

ABSTRACT. The hydrolytic degradation of squaramides and squaramic acids, the product of partial hydrolysis of squaramides, has been evaluated by UV spectroscopy at 37°C in the pH range 3-10. Under these conditions, the compounds are kinetically stable over long time periods (>100 d). At pH > 10, the hydrolysis of the squaramate anions shows first-order dependence on both squaramate and OH^-. At the same temperature and $[OH^-]$, the hydrolysis of squaramides usually displays biphasic spectral changes (A → B → C kinetic model) with formation of squaramates as detectable reaction intermediates. The measured rates for the first step ($k_1 \sim 10^{-4}$ $M^{-1}s^{-1}$) are two to three orders of magnitude faster than the second one ($k_2 \sim 10^{-6}$ $M^{-1}s^{-1}$). Experiments at different temperatures provide activation parameters with values of $\Delta H^{\ddagger} \sim 9 - 18$ kcal mol^{-1} and $\Delta S^{\ddagger} \sim (-5) - (-30)$ cal K^{-1} mol^{-1}. DFT calculations show that the mechanism for the alkaline hydrolysis of squaramic acids is quite similar to that of amides.

Introduction

3,4-Diamino derivatives of squaric acid, also known as squaramides, have received increasing attention in recent years.[1] Owing to their small size and relatively easy preparation, squaramides have found applications in diverse areas of chemistry such as molecular recognition,[2] supramolecular catalysis[1d,3,4] materials science,[5] ion and molecular transport,[6] and sensing.[7] In the biological realm, squaramides have been used for specific cell labelling,[8] to prepare active bioconjugates,[9] or to replace the phosphate and amide-type groups in bioisosteric replacements.[10] In medicinal chemistry, cell-penetrating squaramides are known to exhibit significant anticancer [11] and antiparasitic activity.[12]

There are evident similarities between squaramides and amides or ureas, the nitrogen atoms of a secondary squaramide are coplanar with the cyclobutendione ring. Their sp^2-hybridisation is evidenced by a N–C(sp^2) bond length of 1.32 Å, which is significantly shorter than the single C(sp^3)–N bond of 1.46 Å (Figure 1A).[13] The measured barrier to rotation around the N–C(sp^2) bond is around 63 kJ mol^{-1}, which give rise to the observation of *Z*,*Z* and *Z*,*E* conformers.[14] Squaramides are also known to show certain aromatic character[5c,15] and enhanced hydrogen bonding capabilities as hydrogen bond donors[16,13] and acceptors [7a,17] all in all resulting in compounds with excellent hydrolytic stability.

Despite the growing uses of squaramides and their unique properties, it is surprising that little is known about the physicochemical events underlying the fate and degradation of squaramide-based compounds.[18] Knowledge of the hydrolytic stability and resistance to chemical degradation of squaramides is a relevant issue, with chemical and biomedical

implications. In particular, a hydrolytic degradation pathway is likely to occur in bioactive squaramides and conjugates as part of the catabolism of these compounds.

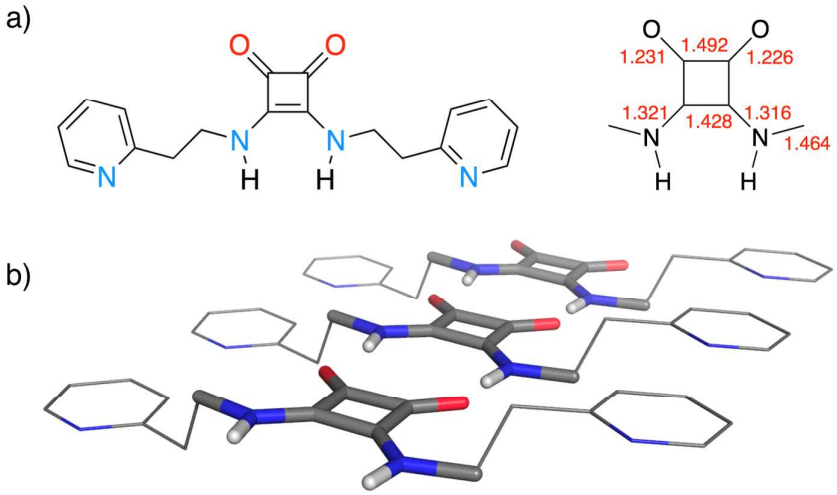

Figure 1. a) X-ray bond lengths (Å) of a squaramide (CCDC 645873)[13] used as model. b) Perspective side-view showing the planar arrangement of the squaramide units in the solid state and the two effective head-to-tail NH•••O=C hydrogen bonds occurring between the squaramide units.

In this work, we have examined the hydrolysis of several squaramides under biological conditions (37 ºC, buffered aqueous solutions, 0.15 M ionic strength, $[H^+]$ or $[OH^-] < 10^{-2}$ M). Nevertheless, the reluctance of these compounds to hydrolysis have led us to strengthen the conditions when necessary ($0.01 < [H^+]$ or $[OH^-] < 1$ M), while keeping the temperature at 37 ºC and raising the ionic strength to 1 M (NaCl).

Results and Discussion

The full hydrolysis of squaramides produces squaric acid and two amines. Nevertheless, 3-hydroxy-4-amino derivatives of squaric acid, also known as squaramic acids, are formed as intermediates during hydrolysis. Hence, the kinetic data from the hydrolysis

of squaramic acids are expected to provide valuable information about the rate law and hydrolysis rates in a simple manner. Furthermore, this allows us to assess the effect of the neighbouring group, i.e. hydroxyl *vs.* amide groups. For this reason, the kinetics of hydrolysis of several squaramic acids as a function of pH has been evaluated before facing the study of squaramides. In all cases, the kinetics were studied under pseudo first order conditions by monitoring the time-dependent changes in the UV-vis spectra of the corresponding squaramic acid or squaramide at 37°C. The experiments were carried out at different pH values, and the apparent rate constants (k_{obs}) were calculated by performing global analyses of the absorption spectra acquired during the hydrolysis.[19]

Scheme 1. Alkaline hydrolysis of squaramic acids.

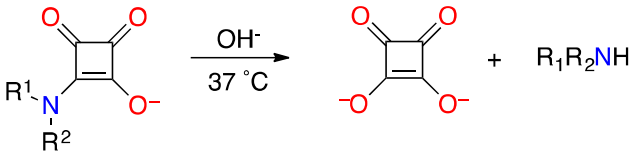

1 R^1 = n-Bu; R^2 = H
2 R^1 = $(CH_2)_3NMe_2$; R^2 = H
3 R^1 = $(CH_2)_3COOH$; R^2 = H
4 R^1 = $(CH_2)_3NMe_2$; R^2 = Me
5 R^1 = Ph; R^2 = H
6 R^1 = R^2 = *i*-Pr

At neutral pH, the squaramic acids **1** – **6** (Scheme 1) show intense absorption bands ($\varepsilon > 2 \times 10^4$ M^{-1} cm^{-1}) in the UV range with maximum absorptions at 276.0, 283.0, 274.0, 290.7, 294.0 and 308.0 nm respectively. Under the same experimental conditions, the spectrum of the hydrolysis product, squaric acid, shows a band at λ_{max} 269.0 nm. Preliminary kinetic experiments showed that spectral changes are negligible when samples of squaramic acids **1** to **4** are incubated at 37 ºC for several days in buffered solutions ranging from pH 4 – 10. Long-term experiments (40, 100, 190 days) carried out in screw-capped vials in the same experimental conditions did not evolve into the

squaric acid either. Hence, it can be deduced that squaramic acids are kinetically stable towards hydrolysis in mild acidic or basic media. However, hydrolysis of squaramic acids **1 –** 4 occurs at 37 ºC within a few days under stronger alkaline conditions ($[OH^-]$ = 0.01 – 1.00 M). The results clearly reveal the formation of the squarate anion in a single kinetic step as depicted in Figure 2a for compound **4** (10^{-5} M, $[OH^-]$ 0.9 M).

The observed rate constants (k_{obs}) show a linear dependence on the concentration of base (Figure 2b), thus excluding the ionisation of the squaramidic NH hydrogen as it would lead to a nonlinear dependence of k_{obs} on the hydroxide ion concentration.[20] The fit of the data to Equation 1 leads to the second order rate constants (k) included in Table 1. This shows that the reactivity of the squaramic acids **1** – **4** is very similar (5.9 – 8.7 × 10^{-6} M^{-1} s^{-1}) regardless of the leaving group. However, compound **5** (R_1 = Ph) exhibits saturation kinetics (equation 2) on hydroxide concentration (Figure 2c), thus implying the existence of an initial acid-base equilibrium, with equilibrium constant K, in which OH^- abstracts a proton from the NH group and form the conjugate base of **5** which is unreactive against hydrolysis. Formation of the squarate anion occurs trough reaction of the unmodified **5** with a rate constant k (equation 2), equivalent to the k defined in equation1.

$$k_{obs} = k[OH^-] \qquad (1)$$

$$k_{obs} = \frac{k[OH^-]}{1 + K[OH^-]} \qquad (2)$$

Equilibrium and rate constants can be obtained from the fitting to Equation 2, and these show a faster hydrolysis rate (k = 63 ± 8 ×10^{-6} M^{-1} s^{-1}) and an equilibrium constant of 9 ± 1 M^{-1}.

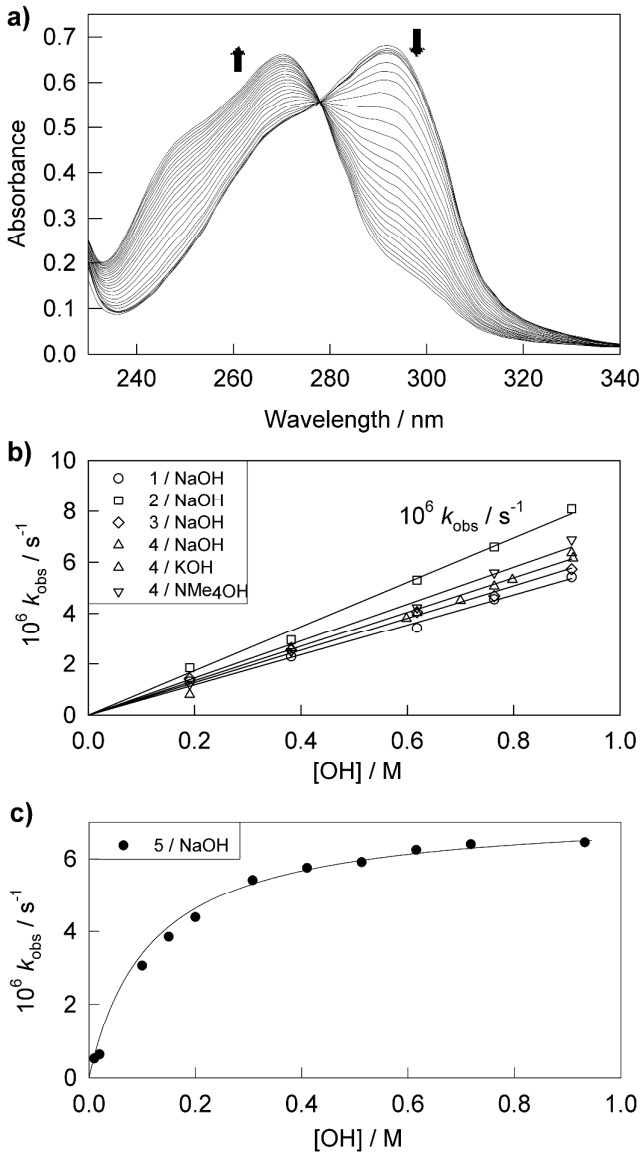

Figure 2. (a) Spectral evolution for the hydrolysis of a 10^{-5} M solution of **4** with 0.9 M NaOH (for clarity only one out of three recorded spectra is shown). (b) k_{obs} vs. [OH] plots for **1** - **4** / NaOH, **4** / KOH and **4** / NMe_4OH. (c) k_{obs} vs. [OH] plot for **5** / NaOH.

A behaviour similar to that of compound **5** has been reported for the alkaline hydrolysis of trichloroacetamide (CCl_3CONH_2) and trifluoroacetanilide ($CF_3CONHPh$), where K corresponds to the equilibrium constant for the ionisation process caused by the

enhanced acidity of these activated amides.[21] Thus, the observed rate equation for **5** can be explained by the formation of its conjugate base as an unreactive side product.[20, 22] Finally, compound **6** does not appreciably hydrolyse under similar experimental conditions.

Table 1. Second order rate constant (*k*) for the alkaline hydrolysis of 1 – 6 at 37 ºC.

Substrate/Base	10^6 x k_2 $M^{1}s^{-1}$
(**1**)/NaOH	5.9 ± 0.1
(**2**)/NaOH	8.7 ± 0.2
(**3**)/NaOH	6.3 ± 0.1
(**4**)/NaOH	6.7 ± 0.2
(**4**)/KOH	6.6 ± 0.1
(**4**)/NMe_4OH	7.3 ± 0.2
(**5**)/NaOH [a]	63 ± 8
(**6**)/NaOH	-

[a] A pre-equilibrium constant of $K = 9 \pm 1$ M^{-1} was measured for this system.

The rate constants for the hydrolysis of compounds **1** – **5** compare well with those reported for standard amides such as acetamide, N-methylacetamide, and N-ethylacetamide, which have alkaline hydrolysis constants of 4.71×10^{-5}, 5.46×10^{-6} and 3.10×10^{-6} M^{-1} s^{-1}, respectively, at 25ºC.[23] Thus, the anionic nature of the starting squaramate anion apparently does not interfere the hydrolysis of the squaramide bond. Additionally, compound **4** was treated with KOH/KCl and NMe_4Cl/NMe_4OH, without a noticeable cation effect.

Chart 1. Chemical structures of the squaramides investigated in this work.

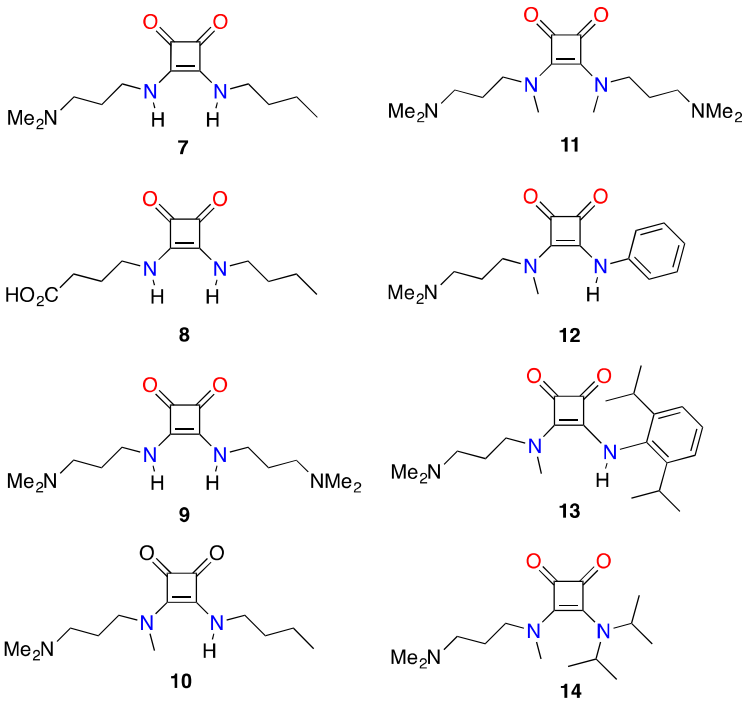

As squaramides derived from simple alkyl or aryl amines are insoluble in water, carbon chains containing solubilising groups such as dimethylamino or carboxylic acid groups were introduced to fulfil this function (Chart 1). The spectra of the squaramides **7** – **14** show the absorption band slightly shifted towards higher wavelengths compared to squaramic acids **1** – **6**, the maximum being now observed in the range of 293 – 313 nm. Long-term experiments were again necessary to follow progress in the hydrolysis of the squaramides at 37 ºC under buffered neutral (pH 4 to 10) and acidic conditions ([HCl] = 0.01 – 0.14 M). Experiments using samples of compound **10** at different pH in sealed vials at 37 ºC and measured after 40, 100 and 190 days only showed small changes at pH 9-10, and even minor changes at pH lower than 2. Therefore, the hydrolysis of bis-

squaramides requires stronger conditions under acidic (pH < 2) than under alkaline conditions (pH > 8).

The alkaline hydrolysis was then studied under conditions similar to those previously used for squaramates. As expected, the spectral changes observed are more complex than those found previously for the squaramates. Those for the hydrolysis of the antichagasic agent **10**,[12b] are included in Figure 3. For compounds **7 – 11**, the evolution of the spectra with time corresponds to biphasic kinetics. The spectral changes are satisfactorily fitted to an A→B→C kinetic model with observed rate constants k_{1obs} and k_{2obs}.

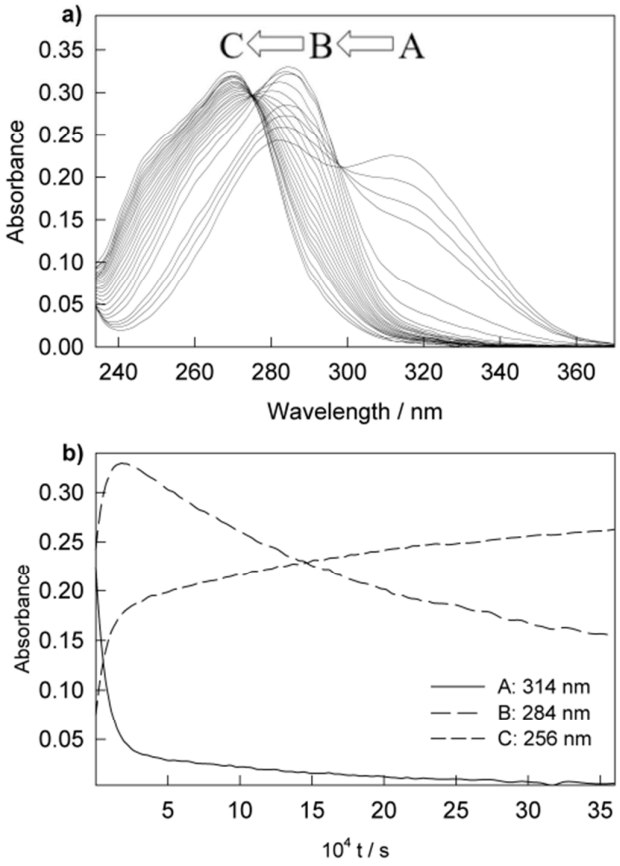

Figure 3. a) Spectral changes with time observed during the hydrolysis of squaramide **10** at 37ºC in NaOH 0.9 M. For clarity, only one out of the three recorded spectra is shown. b) Selected traces at various wavelengths.

The rates of both steps vary with the concentration of base, but the dependence is different in both cases. In the first step, saturation kinetics is observed (Figure 4a), and k_{1obs} values fit equation 2. The exception is compound **11**, lacking any ionisable NH group, for which k_{1obs} increases linearly with [OH^-] and the values can be fitted to equation 1 (Figure 4b). In the second step, k_{2obs} values satisfactorily fit equation 1 and yield the second order hydrolysis rate constants k_2 included in Table 2.

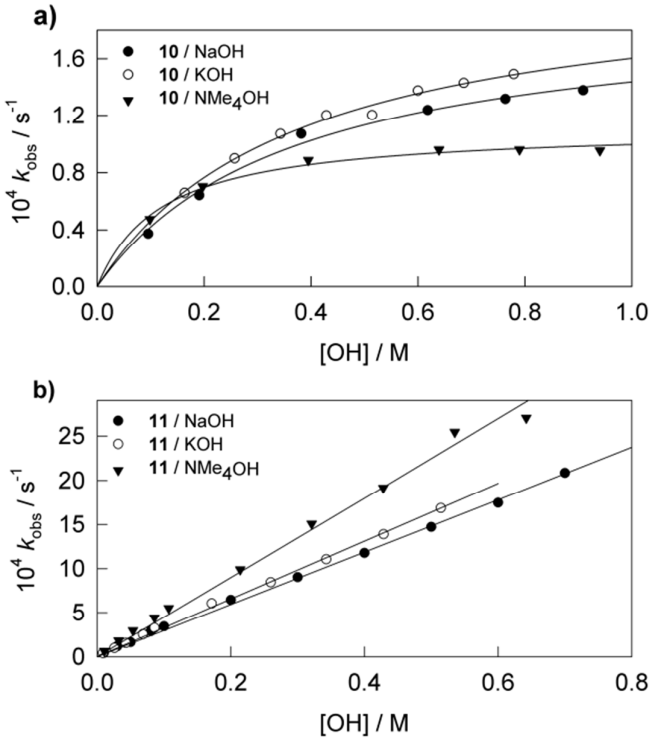

Figure 4. Plot of [OH^-] *vs.* k_{1obs} for the hydrolysis of **10** (a) and **11** (b) in the presence of different salt/base combinations.

The values of k_1, K and k_2 for squaramides **7 – 14** are included in Table 2. Remarkably, the alkaline hydrolysis of trichloroacetamides, acetamides, and N-phenyl ureas, among others,[21a,23,24] show a nonlinear relationship between k_{1obs} and [OH^-] similar to that

observed for **5**. The saturation kinetics observed in those cases is explained by the ionisation of the NH groups of the amides or ureas, leading to unreactive conjugate bases at high pH. A similar interpretation is possible in the present case, the nature of the pre-equilibrium responsible for the saturation kinetics at high hydroxide ion concentration for **7** – **10** (and also for squaramate **5**) is likely related to the ionisation of the squaramides bearing N-H groups (Scheme 2). The different rate-law observed for **11**, which lacks NH groups and showed a linear dependence on [OH^-], gives further support to this interpretation.

The rate constants for the second resolved step match well with those obtained for the squaramate hydrolysis, with values around 6×10^{-6} $M^{-1}s^{-1}$. A comparison between the first and second hydrolysis rate constants shows that the first hydrolysis step is roughly two to three orders of magnitude faster than the second one ($k_1 >> k_2$). This effect is similar to the known difference in reactivity observed for the alkaline hydrolysis of phosphate triesters compared to anionic phosphate diesters.[24] The relative hydrolysis rates of certain diamides also show a similar trend. For instance, the alkaline hydrolysis of *cis*-maleamide at 65 ºC is greater than that for acetamide by two orders of magnitude[25] with the enhanced reactivity being explained based on the electron-withdrawing ability of a second amide group. However, the same argument cannot be employed to explain the differences observed between squaramides and squaramate anions. Instead, it appears that the different rates of hydrolysis of the two-squaramide groups have an electrostatic origin. The squaramate anion formed after the first hydrolysis has more difficulties to react readily with hydroxide or hydroxide-water cluster anions because of the electrostatic repulsion between the two-negatively charged ions.

Table 2. Kinetic Parameters for the Alkaline Hydrolysis (NaOH) of Squaramides 7– 14.

Substrate [a]	$10^4 \times k_1$ M^{-1} s^{-1}	K M^{-1}	$10^6 \times k_2$ M^{-1} s^{-1}	k_1/k_2
7	3.42 ± 0.02	3.98 ± 0.04	7.04 ± 0.05	49 ± 0.6
8	2.6 ± 0.2	3.2 ± 0.4	6.22 ± 0.09	42 ± 4
9	3.7 ± 0.2	4.6 ± 0.3	8.25 ± 0.05	45 ± 3
10	5.4 ± 0.5	2.7 ± 0.4	6.4 ± 0.2	84 ± 10
11	29.7 ± 0.3		6.57 ± 0.07	452 ± 9
12	0.141±0.001			
13	0.004[b]			
14	15.1 ± 0.2			

[a] The kinetic measurements were carried out at 37°C on 10^{-5} M solutions of the corresponding squaramides in H_2O (1M NaCl). [b] The value of the rate constant for **13** is an estimation based on the NMR observations.

The k_1/k_2 ratios for compounds **7**, **8** and **9** are all close to 50 whereas compound **10** shows ratios between 84 and 114, with the value increasing with the size of the cation ($Na^+ < K^+ < NMe_4^+$)(Supporting Information). Compound **11** exhibits the greatest effect (452 for Na^+ and 612 for NMe_4^+). All in all, it seems that the presence of tetramethylammonium cations accelerates the first hydrolysis step in relation to the second one.

The introduction of aromatic substituents in compounds **12** and **13** provides an additional stabilization of charged species by both the cyclobutene and phenyl rings. The formation of an imidate anion makes compound **12** to evolve much more like a squaramic acid in terms of hydrolysis rate. Besides, the hydrolysis is directed towards the aliphatic amine group in spite of its slower hydrolysis, which is then followed by a fast aniline release in the second hydrolysis step.

Scheme 2. Two-step alkaline hydrolysis of a representative squaramide.

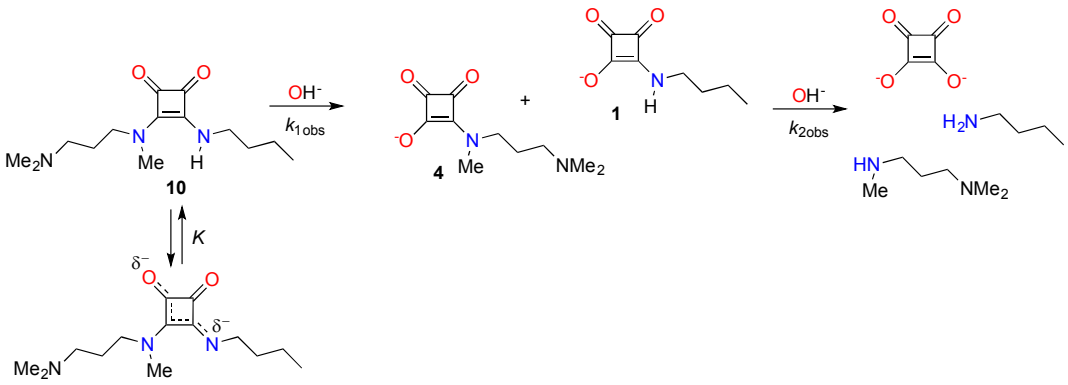

An interesting aspect that deserves attention is the regioselectivity of the hydrolysis in unsymmetrical squaramides. The global analysis of the kinetic data is very useful in this regard, as it provides a calculated spectrum for the reaction intermediate that can be compared with the experimental spectra of the two possible squaramates. For instance, the calculated spectrum of the putative intermediate appearing during the alkaline hydrolysis of **10** shows a maximum at λ_{max} = 285.5 nm and therefore does not coincide with any of the two available options, squaramates **1** (λ_{max} = 276 nm) or **4** (λ_{max} = 290.7 nm). This observation indicates that the recorded spectrum must be a combination of the spectra of these two squaramates (Figure S1). Their relative abundances can actually be obtained by fitting the calculated spectrum to a linear combination of them, and the results indicate that the mixture is composed of 31% of **1** and 69% of **4**.

NMR experiments performed on the squaramide **10** (0.9 M NaOD/D_2O, 37 °C, 6 h) confirmed the formation of a mixture of squaramates as intermediates in the alkaline hydrolysis of unsymmetrical squaramides. Under these conditions, the concentration of the squaramate intermediates approaches a maximum. The resulting ^{1}H-NMR spectrum matches well with the superposed spectra of **1**, **4** and the corresponding free amines (Figure S2). The integration of the characteristic squaramide NCH_2 signals (δ 3.25 –

3.50 ppm in alkaline conditions) provides a value of 55:45 for the **1**:**4** ratio, in reasonable agreement with the previous kinetic results. Although both approximations do not agree in which is the dominant intermediate, it is clear that the rate constants for the hydrolysis of both C-N bonds are quite similar and that there is no preferred pathway for the first hydrolysis step. Regarding the hydrolysis of the squaramates, their rates are quite similar and in the second kinetic step, the mixture of **1** and **4** would react with rate constants of 5.9×10^6 and 6.7×10^6 M^{-1} s^{-1}, respectively (see Table 1). However, because of the similarity between both constants, a single averaged value of 6.4×10^6 M^{-1} s^{-1} is observed for the second kinetic step in the hydrolysis of **10**.

In marked contrast to squaramides **7** – **11**, the hydrolysis of compound **12** takes place with monophasic kinetics, yielding the squarate dianion without any observable intermediate (Figure S3). The spectral changes can be fitted to an A→B kinetic model, and the k_{1obs} *vs.* [OH] plot shows a linear dependence on the hydroxide concentration (Equation 1) with $k_1 = (1.41 \pm 0.01) \times 10^{-5}$ M^{-1} s^{-1}. NMR monitoring of the reaction in D_2O/NaOD confirms the absence of detectable intermediates. These results suggest that the hydrolysis of **12** takes place first at the aliphatic amine side (slow process) and then at the aniline group (fast), as indicated in Scheme 3. This hypothesis is further supported by the fact that the value of the rate constant for **5** in Table 1 is larger than the value of k_1 for **12** in Table 2. The hydrolysis kinetics of **12** is closer to that of the related squaramate **4** (aliphatic residue, $k = 0.67 \times 10^{-5}$ M^{-1} s^{-1}, Equation 1) than to that of **5** (aromatic residue, $k = 6.3 \times 10^{-5}$ M^{-1} s^{-1}, Equation 2).

Compound **13** represents another exception to the general behaviour of squaramides. The introduction of two ^{i}Pr groups in the *ortho* positions of the aniline substituent effectively hinders the hydrolysis at both sides of the molecule, which remains unaltered under similar conditions and time frame (i.e. [OH] = 0.1 – 0.9 M, 37 ºC and 5.5 days).

After three weeks, NMR experiments show that only 20% of **13** is partially hydrolysed at the aliphatic amine side, similarly to compound **12** but much slower. In agreement with the expectations from the behaviour of other compounds, squaramide **14** undergoes hydrolysis at only one position to yield squaramate **6**, which is reluctant to hydrolysis under identical conditions when studied separately. The process takes places in a single kinetic step with observed rate constants linearly dependent on the [OH^-].

Scheme 3. Alkaline hydrolysis of the phenyl substituted squaramide 12.

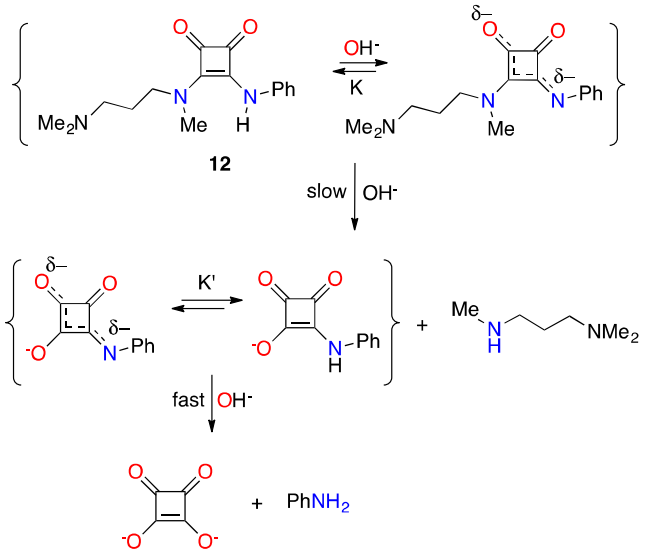

Variable temperature kinetic experiments allowed obtaining the activation parameters ($\Delta H^{\ddagger}$ and $\Delta S^{\ddagger}$) and the standard enthalpy and entropy of the pre-equilibrium using Van't Hoff plots. Table S1 summarises the activation parameters for compounds **7**, **9**, **10**, and **11**. The results ($\Delta H^{\ddagger}$ ~ 12 – 16 kcal mol^{-1}, $\Delta S^{\ddagger}$ ~ (-19) – (-31) cal K^{-1} mol^{-1}), are similar to those reported for a series of diamides ($\Delta H^{\ddagger}$ ~ 9 – 18 kcal mol^{-1}, $\Delta S^{\ddagger}$ ~ (-5) – (-30) cal K^{-1} mol^{-1}), namely oxalamide, malonamide, succinamide and *cis/trans*-maleamide.[25] This gives further support to the possibility of squaramides and amides sharing a similar

hydrolysis mechanism with formation of steady-state tetrahedral intermediates as INT in Scheme **4.**[26]

Scheme 4. Structure of the tetrahedral intermediate (INT) formed upon OH^- attack.

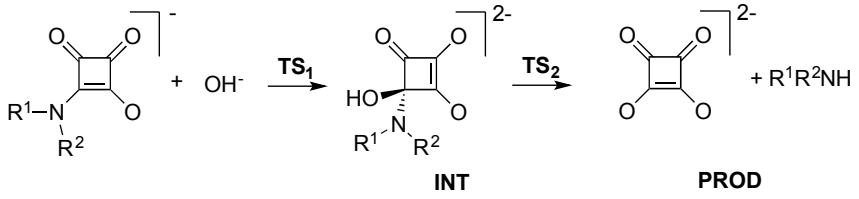

DFT studies. While the hydrolysis of amides has been extensively studied from a computational viewpoint,[27] to our knowledge the mechanism of hydrolysis of squaramides and squaramic acids has never been analysed in depth.[5c,28] Thus, to gain insight into the mechanism of the hydrolysis of squaramides we carried out DFT calculations at the M06-2X//cc-pVTZ/PCM level of theory (for further information see Supporting Information). We initially assumed that the alkaline hydrolysis of squaramates takes place *via* the tetrahedral intermediates II formed when the hydroxide anion attack the C4 position of a squaramate anion.[29]

The calculations on compounds **1** and **6**, featuring secondary and tertiary alkyl amine groups, respectively, only led to minor structural and energetic differences. These results were further confirmed by computing the hydrolysis of the model compounds **1t** and **6t**, in which the alkyl chains were replaced by methyl groups (Table S2 and Figure S4). In all these cases, the initial formation of the tetrahedral intermediates (**INT**) is thermoneutral (ΔG_{INT} ~ 0 kcal mol^{-1}), taking place with barriers of ca. 13 – 15 kcal mol^{-1} (**TS_1**). The C_4□N bond breaking occurs in a subsequent step that is concerted with the proton transfer from the hydroxyl ligand to the departing amine (see **TS_2(1)** in Figure S4). This step is rate-determining and takes place with barriers of ca. 30 kcal mol^{-1}.

It is worth noting that the structures thus computed for the hydrolysis of **1**, **1t**, **6** and **6t**, are analogous to those calculated for the hydrolysis of amides.[27c] Especially relevant are those of the rate-determining second step (**TS_2**), all featuring additional four-membered rings due to the O–H···N interaction that allows the O-to-N proton transfer to be concerted with the C–N bond cleavage. Computational studies of the alkaline amide hydrolysis have shown that an ancillary water molecule, hydrogen bonded to the tetrahedral intermediate, significantly decreases this **TS_2** barrier. The molecule of water acts as a bridge that facilitates the step due to the formation of more stable six-membered ring transition states.[27] Importantly, a similar effect is observed when the alkaline hydrolysis of **1**, **1t**, **6** and 6t is computed in the presence of an explicit H_2O molecule. The associated energy values are included in Table 3, whereas Figure 5 shows the relevant structures for the hydrolysis of **1**•H_2O.

Table 3. Computed relative Gibbs free energies of the minima and transition states involved in the hydrolysis of squaramates including an explicit water molecule. Values are given in kcal mol^{-1}.[a]

Substrate	**HBA**	**TS_1**	**INT**	**TS_2**	**PROD**
1·H_2O	-12.6	5.5	-7.2	9.8	-34.8
1t·H_2O	-12.2	4.9	-7.3	8.8	-34.9
6·H_2O	-13.4	11.9	3.6	13.6	-35.1
6t·H_2O	-13.8	4.6	-5.6	9.1	-32.4
5·H_2O	-11.7	3.9	-7.6	5.2	-37.0
10t·H_2O-A[b]	-15.7	5.9	-20.6	-7.8	-42.5
10t·H_2O-B[b]	-15.7	-6.8	-21.0	-8.3	-45.0

[a] Hydroxide anion and H-bonded [squaramate···OH_2] species are the reactants, whereas the released amine and [squarate···OH_2] species are computed as products. [b] The labels A and B correspond to the two alternative OH^- attacks on C3 or C4 carbons of model squaramide **10t**, respectively.

The interaction between hydroxide and the hydrated squaramates leads to the formation of H-bonded adducts (**HBA**) that are ca. 12 – 15 kcal mol^{-1} more stable than the separated reactants. From these adducts, it is possible to generate the tetrahedral intermediates **INT** with $\mathbf{TS_1}$ barriers of ca. 18 kcal mol^{-1}, except for **6** that shows a barrier of 25.3 kcal mol^{-1}. As expected, the explicit H_2O does not have an active role in the initial step of the hydrolysis, i.e. it is only H-bonded to the squaramate throughout the step, and therefore the barriers are close to those in Table S2, again except for **6**.

In contrast, the data in Table 3 show that the inclusion of an explicit H_2O molecule in the calculations decreases the barrier for the second step of the hydrolysis significantly. At this level of theory, the hydrolysis ($\mathbf{TS_2}$) adopts barriers of 10 – 17 kcal mol^{-1} (cf. 30 kcal mol^{-1} in the absence of the H_2O molecule). Such stabilisation can be explained based on the combination of that due to the H-bonding interactions, also appearing during the first step of the process, and the above-mentioned catalyst effect of H_2O, which serves as a proton bridge and facilitates the concerted O-to-N proton transfer. The computed structure of $\mathbf{TS_2(1}\cdot H_2O\mathbf{)}$ in Figure 5 clearly exemplifies this catalytic role by presenting H···O distances between the hydroxyl group and the water molecule of 1.15 and 1.29 Å, indicative of an ongoing proton transfer process. Notably, the marked decrease in the computed $\mathbf{TS_2}$ barriers makes the formation of the tetrahedral intermediates ($\mathbf{TS_1}$) rate-determining in agreement with the experimental results.

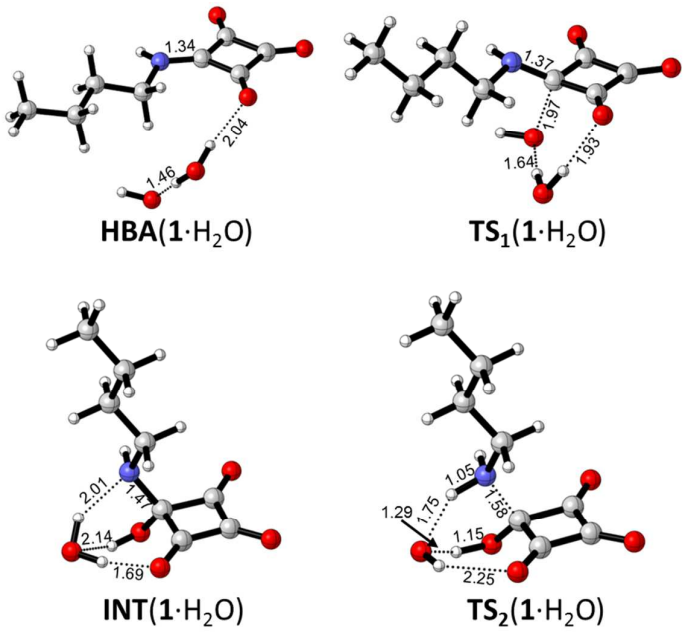

Figure 5. Perspective view of the DFT-optimized structures (M06-2X//cc-pVTZ/PCM) of **HBA(1**·H_2O), **TS_1(1**·H_2O**)**, **INT_1(1**·H_2O**)** and **TS_2(1**·H_2O**)**. Distances are given in Å.

Interestingly, the overall computed barrier for the alkaline hydrolysis of squaramate **6** is 27.0 kcal mol^{-1}, i.e. significantly larger than those of **1**, **1t** and **6t**, and in agreement with the experimental observation of hindered hydrolysis of this compound. These thermochemical changes can be understood by the presence of the bulkier $N(^{i}Pr)_2$ amine. Specifically, the two ^{i}Pr chains in **TS_2(6**·H_2O**)** (Figure S5) preclude the H-bonding interaction between the ancillary water molecule and the O atom at one of the neighbouring C–O groups (d(H···O)= 2.25 Å).

Squaramate **5** (R_1 = Ph), whose alkaline hydrolysis also differs from that of **1** (R_1 = nBu), has been modelled both in the absence and presence of an ancillary H_2O molecule. The resulting free energies (Tables S2 and Table 3) show similarities with those of compounds **1** and **6**. However, a crucial difference appears regarding the barrier for the second step. In the absence of explicit H_2O molecules, the thermodynamic

differences between **TS_2(5)** and **TS_2(1)** follow the general trend, **TS_2(5)** is 14.7 kcal mol^{-1} above the separated reactants whereas the value for **TS_2(1)** is 28.6 kcal mol^{-1}. As a consequence, the overall **TS_2** barrier for squaramate **5** is only 16.1 kcal mol^{-1}. Comparison of the structures of **TS_2(5)** (Figure S6), and **TS_2(1)** (Figure S4) allows to trace the origin of the effect to the absence in **TS_2(5)** of the above-mentioned O-H···N interaction (d(H···N)= 2.83 Å, cf. 1.74 Å in **TS_2(1)**) that results in the four-membered ring required for the O-to-N proton transfer to be concerted with the C–N bond cleavage.[30] Here, the lower basicity of aniline compared to other departing amines,[31] make the concerted O-to-N proton transfer not required for the C□N bond cleavage to take place. As a consequence, the inclusion of a water molecule to model the alkaline hydrolysis of **5** does not result in the drastic thermodynamic changes computed for **1**, **1t**, **6** and **6t**. Nonetheless, in line with the relatively fast alkaline hydrolysis of **5** (see Table 1), the calculated **TS_1** barrier for this compound in the presence of one explicit H_2O molecule is 15.9 kcal mol^{-1}, i.e. 2-3 kcal mol^{-1} lower than those for **1**, **1t**, **6** and **6t** (Table 3).

The hydrolysis of the squaramides was computationally analysed subsequently. Experimental work on the squaramide **10** has shown that the process involves the formation of two intermediates (squaramates **1** and **4**) with comparable rate constants and, therefore, they both should be formed with relatively similar barriers. To confirm this hypothesis, we computed the two possible pathways for the first hydrolysis in alkaline media of the model compound **10t** in the presence of one explicit H_2O molecule.

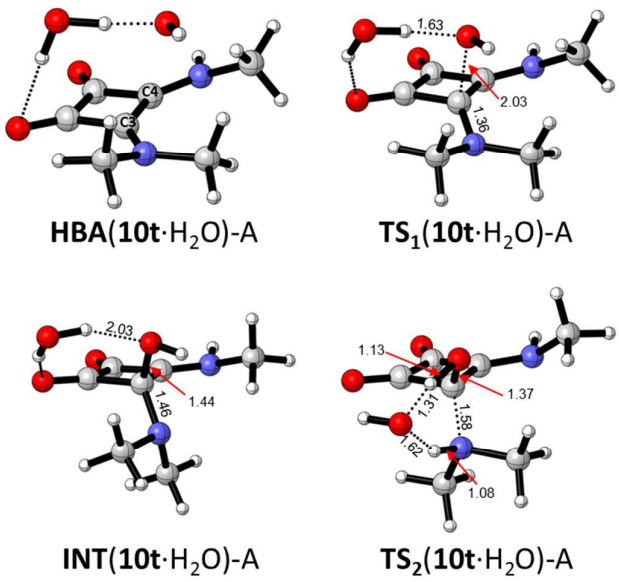

Figure 6. Perspective view of the DFT-optimized structures (M06-2X//cc-pVTZ/PCM) of **HBA**(**10t**·H_2O)-A, **TS$_1$**(**10t**·H_2O)-A, **INT$_1$**(**10t**·H_2O)-A and **TS$_2$**(**10t**·H_2O)-A. Alkyl groups were replaced by methyl groups. Distances are given in Å.

Similarly to the results for the alkaline hydrolysis of squaramates, the interaction of **10t**·H_2O with hydroxide leads to the formation of an H-bonded adduct **HBA**(**10t**·H_2O) that is 15.7 kcal mol^{-1} more stable than the separated reactants (see Figure 6). The attack of a hydroxide can take place subsequently either at the C3 or C4 positions of this squaramide, ultimately leading to the formation of the squaramates **1t** and **6t**, respectively. These two pathways have been labelled as A and B, respectively. The corresponding thermodynamic data are included in Table 3 whereas Figure 6 shows the structures computed for pathway A. The data indicate that the free energy profiles for pathways A and B are almost identical. Indeed, the **TS$_1$** barriers are 9.8 and 8.9

kcal/mol, respectively, whereas those for the second step ($\mathbf{TS_2}$) are 12.9 and 12.7 kcal/mol, respectively. These minor differences are surely within the computation errors, and so, the calculations suggest that the products resulting from both pathways, i.e. squaramates **1t** and **6t**, should both be observed as the products of the partial hydrolysis of **10t**. These observations give support to the initial hypothesis of the first alkaline hydrolysis of **10** not being regioselective, i.e. leading to a mixture of squaramates **1** and **6**. From a structural viewpoint, comparison of the geometries for the first alkaline hydrolysis of **10t**·H_2O in Figure 6 and that of **1**·H_2O in Figure 5 shows little geometrical differences associated with the nature of the substituent at the adjacent carbon atom. The electronic consequences of this structural change are, however, significant as the $\mathbf{TS_1}$ and $\mathbf{TS_2}$ barriers in **10t**·H_2O are significantly lower than those for **6t**·H_2O, in agreement with the first hydrolysis of squaramides being two to three orders of magnitude faster than the second one.

Conclusions

All in all, the studied squaramides and squaramate anions are kinetically stable at a temperature of 37 °C and pH range of 2 to 8. At pH above 8 the hydrolysis of these compounds become observable. The present results demonstrate that the alkaline hydrolysis of squaramate anions proceeds with second order kinetics, and that the hydrolysis is relatively slow ($k \approx 10^{-6}$ $M^{-1}s^{-1}$) and unaffected by the existence of potentially interacting groups such as dimethylamino or carboxylate groups. On the other hand, the rate constants for the hydrolysis of the squaramides take place in two kinetically distinct steps. The first step ($k_1 \approx 10^4$ M^{-1} s^{-1}) is ca. 10^2 times faster than the second one ($k_2 \approx 10^{-6}$ M^{-1} s^{-1}), with the latter values being comparable to those obtained for the corresponding squaramates. This general trend is not unexpected since the

second hydrolysis step of squaramides occurs on negatively charged squaramate anions. On these premises, and given the resemblance with the alkaline hydrolysis of amides[26] a mechanism involving the formation of tetrahedral intermediates through the nucleophilic attack of a hydroxide ion to the C3 and C4 carbons of the squaramides can be proposed. This mechanism is supported by DFT calculations using a continuum-discrete solvation model. In addition to the kinetic and mechanistic details, the present results demonstrate the kinetic stability of squaramic acids and squaramides in aqueous solutions in a broad range of pH and must be useful to anyone planning to use them in the near future.

Experimental Section

The various chemicals were of commercial origin (Aldrich or Scharlau) and used as received. ^{1}H, ^{13}C and 2D NMR spectra (at 300 and 600 Mhz) and ^{13}C (at 75 and 150 MHz) spectra were recorded on 300 and 600 MHz spectrometers in $CDCl_3$ or d_6-DMSO solutions at room temperature. The residual proton signal was used as reference. Chemical shifts (δ) are given in ppm and coupling constants (J) in Hz. ESI-HRMS mass spectra were recorded on magnetic sector or on Orbitrap mass spectrometers. Elemental analyses (C, H, N) were conducted by the "Centro de Microanálisis Elemental" of the "Universidad Complutense de Madrid" (Spain).

Synthesis: The squaramic acids **1** – **4** and **6** were prepared by hydrolysis of the corresponding ethyl esters. Squaramic acid **5** was prepared according to a reported procedure.[32] The squaramides **7** to **11**, were previously synthesized according to a modified procedure.[12b] Squaramides **12** – **14** are new compounds.

Typical procedure for the preparation of the squaramic acids 1 – 6

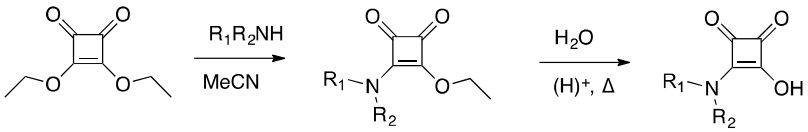

1a R_1= *n*-Bu; R_2 = H
2a R_1= $(CH_2)_3NMe_2$; R_2 = H
3a R_1= $(CH_2)_3COOH$; R_2 = H
4a R_1= $(CH_2)_3NMe_2$; R_2 = Me
5a R_1= Ph; R_2 = H
6a R_1= R_2 = *i*-Pr

1 R_1= *n*-Bu; R_2 = H
2 R_1= $(CH_2)_3NMe_2$; R_2 = H
3 R_1= $(CH_2)_3COOH$; R_2 = H
4 R_1= $(CH_2)_3NMe_2$; R_2 = Me
5 R_1= Ph; R_2 = H
6 R_1= R_2 = *i*-Pr

Diethyl squarate (500 mg, 2.94 mmol) in MeCN (3 mL) and one equivalent of the corresponding amine were mixed in an oven-dried round bottom flask. The mixture was stirred under nitrogen at room temperature (**1a**, **2a)** for 10 h or at higher temperatures for a variable period (see below). The crude mixture was then concentrated under reduced pressure and purified by column chromatography on silica gel eluting with CH_2Cl_2/MeOH (95:5 v/v), or CH_2Cl_2-EtOAc (90/10 v/v) to afford the squaramic acid ethyl esters **1a** – **6a**. Next, the esters (500 mg) were digested with water at 90 °C for 8 to 20 h (Milli-q, 15 – 20 mL), with or without added acid, recovering the resulting solid acids **1 – 4**, **6** by filtration.

*3-(butylamino)-4-ethoxycyclobut-3-ene-1,2-dione (**1a**)*.[14] White amorphous solid 562 mg, yield 97%. mp 49-50 ºC. ^{1}H NMR ($CDCl_3$) δ 6.42 (br s, 0.74H), 5.32 (br s, 0.26H), 4.76 (q, J = 6.9 Hz, 2H), 3.65(br, 0.58H), 3.42(br q, J = 6.6 Hz, 1.53H), 1.59 (m, 2H), 1.44 (t, J = 6.9 Hz, 3H), 1.36(m, 2H), 0.92 (t, J = 7.2 Hz, 3H). ^{13}C NMR ($CDCl_3$) δ 189.9, 182.8, 177.6, 172.6, 69.8, 44.8, 32.8, 19.7, 16.0, 13.8. ESI(+)-HRMS *m/z* (%) calcd for $C_{10}H_{15}NO_3Na$ $[M+Na]^+$ 220.0941; found 220.0936.

*3-((3-(dimethylamino)propyl)amino)-4-ethoxycyclobut-3-ene-1,2-dione (**2a**)*.[14] Yellow amorphous solid 599 mg, yield 90%. mp 56-59 ºC. ^{1}H NMR ($CDCl_3$) δ 7.76 (br s, 0.6H), 7.58 (br s, 0.4H), 4.73 (q, J = 6.9 Hz, 2H), 3.78 (br t, 0.7H), 3.54 (br t, J=6 Hz, 1.3H), 2.43 (br t, J = 5.7 Hz, 2H), 2.22 (s, 6H), 1.73 (m, 2H), 1.42 (t, J = 6.9 Hz, 3H).

^{13}C NMR ($CDCl_3$) δ 189.5, 183.2, 177.3, 172.6, 69.6, 58.8, 58.3, 45.4, 44.9, 26.8, 16.9. ESI(+)-HRMS *m/z* (%) calcd for $C_{11}H_{19}N_2O_3$ $[M+H]^+$ 227.1390; found 227.1389.

*4-((2-ethoxy-3,4-dioxocyclobut-1-en-1-yl)amino)butanoic acid (**3a**)*.[38] To a solution of diethyl squarate (500 mg, 2.94 mmol) and 4-aminobutiric acid (313 mg, 2.94 mmol) in MeCN (10 mL), was added DIPEA (1.05 mL). The mixture was stirred at 50°C for 15 h. The crude was concentrated and diluted with water 12 mL and HCl 3N (3 mL). The resulting solution was extracted with EtOAc (10 × 10 mL). The combined EtOAc extracts were washed with brine, and dried over Na_2SO_4. The solvent was removed under reduced pressure to give a yellow solid 599 mg, yield 90 %. mp 56-59 °C. ^{1}H NMR ($CDCl_3$) δ 7.76 (br s, 0.6H), 7.58 (br s, 0.4H), 4.73 (q, J = 6.9 Hz, 2H), 3.78 (br t, 0.7H), 3.54 (br t, J = 6 Hz, 1.3H), 2.43 (br t, J = 5.7 Hz, 2H), 2.22 (s, 6H), 1.73 (m, 2H), 1.42 (t, J = 6.9 Hz, 3H). ^{13}C NMR ($CDCl_3$) δ 189.5, 183.2, 177.3, 172.6, 69.6, 58.8, 58.3, 45.4, 44.9, 26.8, 16.0. ESI(–)-HRMS *m/z* (%) calcd for $C_{10}H_{12}NO_5$ $[M–H]^–$ 226.07210; found 226.0717; ESI(+)-HRMS *m/z* (%) calcd for $C_{10}H_{13}NO_5Na$ $[M+Na]^+$ 250.06859; found 250.0682.

*3-((3-(dimethylamino)propyl)(methyl)amino)-4-ethoxycyclobut-3-ene-1,2-dione (**4a**)*.[12b] To a solution of diethyl squarate (500 mg, 2.94 mmol) in MeCN (15 mL) were added N,N, N'-trimethyl-1,3-propanediamine 341,6 mg (2.94 mmol). The mixture was stirred at room temperature for 3 h. The crude was concentrated and the residue purified by column chromatography (Silica gel, CH_2Cl_2/MeOH (80/20 v/v) to give a yellow oil 692 mg, yield 98 %. ^{1}H NMR ($CDCl_3$) δ 4.76 (q, J = 7.2 Hz, 1H), 4.75 (q, J = 7.2 Hz, 1H), 3.72 (t, J = 7.2 Hz, 1H), 3.44 (t, J = 7.2 Hz, 1H), 3.34 (s, 1.5H), 3.15 (s, 1.5H), 2.33 (m, 2H), 2.24 (s, 3H), 2.22 (s, 3H), 1.81 (m, 2H), 1.45 (t, J = 7.2 Hz, 1.5 H), 1.44 (t, J = 7.2 Hz, 1.5 H) ppm. ^{13}C NMR (75 MHz, $CDCl_3$) δ 188.3, 188.0, 181.5, 175.6, 175.5,

171.65, 171.3, 68.7, 55.4, 49.7, 49.0, 44.4, 36.0, 35.6, 25.0, 24.8, 15.2 ppm. ESI(+)-HRMS *m/z* (%) calcd for $C_{12}H_{21}N_2O_3Na$ $[M+H]^+$ 241.1552; found 241.1557.

*3-(ethoxy)-4-(phenylamino) cyclobut-3-ene-1,2-dione (**5a**)*.[39] To a solution of diethyl squarate (500 mg, 2.94 mmol) in MeCN (15 mL) was added aniline (275 mg, 2.95 mmol). The mixture was stirred at 80°C for 24 h to give a yellow-orange solid which was isolated by filtration. The crude solid was digested at room temperature with hexane-ethanol (92/8 v/v; 20 mL) and hexane (2 × 20 mL) and filtered to give a yellow solid 500 mg, yield 78 %. mp 111-114 °C. ^{1}H NMR ($CDCl_3$) δ 8.04 (br s, 1H), 7.32 (m, 4H), 7.15 (m, 1H), 4.88 (q, J = 7.2 Hz, 2H), 1.50 (t, J = 7.2 Hz, 3H). ^{13}C NMR ($CDCl_3$) δ 189.0, 184.1, 178.3, 168.8, 137.2, 129.7, 125.1, 119.5, 70.6, 16.1.

*3-(diisopropylamino)-4-ethoxycyclobut-3-ene-1,2-dione (**6a**)*.[40] To a solution of diethyl squarate (500 mg, 2.94 mmol) in MeCN (15 mL) were added N,N-diisopropylamine (598 mg, 5.90 mmol) and DIPEA (1.05 mL). The mixture was stirred at 50°C for 24 h. The crude was concentrated and the residue purified by column chromatography (Silica gel) to give a yellow solid 630 mg, yield 95 %. mp 77-79 °C. ^{1}H NMR ($CDCl_3$) δ 4.82 (q, J = 7.2 Hz, 2H), 4.63 (br m, 1H), 3.93 (m, 1H), 1.45 (t, J = 7.2 Hz, 3H), 1.29 (d, J = 6.6 Hz, 6H) + 1.28 (d, J = 6.9 Hz, 6H). ^{13}C NMR ($CDCl_3$) δ 189.1, 182.6, 175.7, 171.3, 69.6, 50.0, 48.8, 22.1, 21.9, 16.1. ESI(+)-HRMS *m/z* (%) calcd for $C_{12}H_{19}NO_3Na$ $[M+Na]^+$ 248.1257; found 248.1252.

*3-(butylamino)-4-hydroxycyclobut-3-ene-1,2-dione (**1**)*.[32] Obtained as the free acid from a mixture of **1a** (500 mg), water (30 mL) and HCl (3N, 1 mL). White solid 367 mg, yield 86%. mp 165 °C (dec.). ^{1}H NMR (DMSO-d_6) δ 8.32 (br t, 1H), 3.38 (q, J = 6.6 Hz, 2H), 1.49 (m, 2H), 1.28 (m, 2H), 0.87 (t, J = 7.2 Hz, 3H). ^{13}C NMR (DMSO-d_6) δ 185.6, 184.9, 183.7, 174.4, 43.7, 32.9, 19.5, 14.0. ESI(–)-HRMS *m/z* (%) calcd for

$C_8H_{10}NO_3$ $[M–H]^-$ 168.06572; found 168.06527. ESI(+)-HRMS *m/z* (%) calcd for $C_8H_{11}NO_3Na$ $[M+Na]^+$ 192.06314; found 192.06311.

*3-((3-(dimethylamino)propyl)amino)-4-hydroxycyclobut-3-ene-1,2-dione (**2**)*. Pale ochre amorphous solid 430 mg, yield 98%. mp 204-207 ºC. ^{1}H NMR (DMSO-d_6) δ 7.16 (t, J = 6.3 Hz, 1H), 3.42 (q, J = 6 Hz, 2H), 3.06 (t, J = 6.9 Hz, 2H), 2.75 (s, 6H), 1.83 (m, 2H). ^{13}C NMR (D_2O) δ 197.2, 191.1, 183.9, 57.6, 45.4, 43.2, 28.5. ESI(+)-HRMS *m/z* (%) calcd for $C_9H_{14}N_2O_3Na$ $[M+Na]^+$ 221.0897; found 221.0887.

*4-((2-ethoxy-3,4-dioxocyclobut-1-en-1-yl)amino)butanoic acid (**3**)*. Obtained from a mixture of **1a** (500 mg), water (30 mL) and HCl (3N, 3 mL). The crude solution was extracted with EtOAc (10 × 10 mL). The combined EtOAc extracts were washed with brine and dried with Na_2SO_4. Removal of the solvent afforded **3** as a white solid 122 mg, yield 28 %. mp 157-159 ºC (dec.). ^{1}H NMR (DMSO-d_6) δ 8.28 (br t, 1H), 3.39 (q, J = 6.3 Hz, 2H), 2.25 (t, J = 7.2 Hz, 2H), 1.74 (m, 2H). ^{13}C NMR (DMSO-d_6) δ 185.2, 184.5, 183.1, 174,0 173.9, 43.0, 30.6, 25.7. ESI(–)-HRMS *m/z* (%) calcd for $C_8H_8NO_5$ $[M–H]^-$ 198.04080; found 198.0401.

*3-((3-(dimethylamino)propyl)(methyl)amino)-4-hydroxycyclobut-3-ene-1,2-dione (**4**)*. Obtained following the general procedure. Then, the crude solid was digested with hot ethyl ether (3 × 15 mL). White solid 433 mg, yield 98 %. mp >250°C (dec.). ^{1}H NMR (D_2O) δ 3.75 (t, J = 6.6 Hz, 2H), 3.29 (s, 3H), 3.23-3.18 (t, J = 7.7 Hz, 2H), 2.91 (s, 6H), 2.13 (m, 2H). ^{13}C NMR (D_2O) δ 196.1, 190.5, 183.0, 57.3, 50.3, 45.4, 38.2, 25.0. ESI(+)-HRMS *m/z* (%) calcd for $C_{10}H_{17}N_2O_3$ $[M+H]^+$ 213.1239; found 213.1238. Anal Calcd for $C_{10}H_{16}N_2O_3$: C, 56.59; H, 7.60; N, 13.20; found: C, 56.10; H, 7.30; N, 13.03.

*3-(hydroxy)-4-(phenylamino) cyclobut-3-ene-1,2-dione (**5**)*. Obtained as described in the literature by MW irradiation of a mixture of squaric acid and aniline.[32]

3-(diisopropylamino)-4-ethoxycyclobut-3-ene-1,2-dione ***(6)***. Crystalline white solid, quantitative yield. mp >210°C (dec). ^{1}H NMR (DMSO-d_6) δ 10.31 (br s, 1H), 4.32 (m, 2H), 1.25 (d, J = 6.9 Hz, 12H). ^{13}C NMR (D_2O) δ 193.7, 189.4, 182.2, 51.8, 23.9; ESI-FTMS *m/z* (%) calcd for $C_{10}H_{16}O_3N$ $[M+H]^+$ 198.1125; found 198.1125. ESI(–)-HRMS *m/z* (%) calcd for $C_{10}H_{14}O_3N$ $[M–H]^–$ 196.0979; found 196.0973. Anal Calcd for $C_{10}H_{15}NO_3$: C, 60.90; H, 7.67; N, 7.10: found C, 60.73; H, 7.43; N, 7.06.

General procedure for the preparation of the squaramic acids 7 – 11

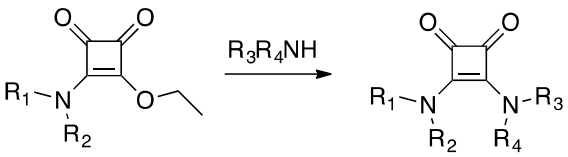

7 R_1 =$(CH_2)_3NMe_2$; R_2=H; R_3= n-Bu; R_4=H
8 R_1=$(CH_2)_3COOH$; R_2=H; R_3 =nBu; R_4=H
9 R_1 =$(CH_2)_3NMe_2$; R_2=H; R_3 =$(CH_2)_3NMe_2$; R_4=H
10 R_1= $(CH_2)_3NMe_2$; R_2 = Me; R_3 =nBu; R_4=H
11 R_1 =$(CH_2)_3NMe_2$; R_2= Me; R_3 =$(CH_2)_3NMe_2$; R_4=Me
12 R_1 = Ph; R_2= H; R_3 =$(CH_2)_3NMe_2$; R_4=Me
13 R_1 =$(iPr)_2$ Ph; R_2=Me; R_3 =$(CH_2)_3NMe_2$; R_4=Me
14 R_1 = iPr; R_2=IPr; R_3 =$(CH_2)_3NMe_2$; R_4=Me

The squaramides **7** – **11** were prepared following a modified procedure described previously by us,[12b] from equimolar mixtures of diethyl squarate (500 mg, 2.94 mmol) and the corresponding R_1R_2NH neat amine or. Alternatively, the above mixture was dissolved in a minimum volume of MeCN or EtOH, and stirred for 3 h at room temperature. After this period, the R_3R_4NH amine (2.97 mmol) was added and the resulting mixture heated further under stirring for several hours. After cooling at room temperature, the crude mixture was purified by column chromatography or by selective precipitation.

3-(butylamino)-4-((3-(dimethylamino)propyl)(methyl)amino)cyclobut-3-ene-1,2-dione ***(7)***.[12b] R_1R_2NH = N,N-dimethyl-1,3-propanediamine (374 μL, 2.94 mmol); R_3R_4NH =

n-butylamine (295 μL, 2.97 mmol). The resulting solid was diluted with MeCN (5 mL), filtered and washed with MeCN (3 × 10 mL). White solid 535 mg, yield 72%.

*4-((2-(butylamino)-3,4-dioxocyclobut-1-en-1-yl)amino)butanoic acid (**8**)*.[12b] R_1R_2NH = 4-aminobutyric acid (313 mg, 2.94 mmol) and DIPEA (1.05 mL, 6 mmol) in MeCN (10 mL) were stirred at 50°C for 8 h. Next, R_3R_4NH = *n*-butylamine (350 μL, 3.5 mmol) was added to the mixture and left stirring at 50°C for 50 h. After solvent removal at vacuo, the residue was dissolved in water and acidified with HCl (1N) to pH 2 to afford **8** as a white solid that was collected by filtration 630 mg, yield 84%.

*3,4-bis((3-(dimethylamino)propyl)amino)cyclobut-3-ene-1,2-dione (**9**)*.[12b] R_1R_2NH = R_3R_4NH = N,N-dimethyl-1,3-propanediamine (860 μL, 6.76 mmol) in 3 mL of EtOH. The mixture was stirred for 15 h at room temperature. After solvent removal at vacuum, the residue was washed with MeCN (3 × 10 mL). White amorphous solid (621 mg, yield 75%).

*3-(butylamino)-4-((3-(dimethylamino)propyl)(methyl)amino)cyclobut-3-ene-1,2-dione (**10**)*.[12b] R_1R_2NH = (N,N,N'-trimethyl-1,3-propanediamine (450 μL, 2.94 mmol); R_3R_4NH = *n*-butylamine (295 μL, 2.97 mmol). CC (neutral Al_2O_3; first CH_2Cl_2, then CH_2Cl_2/MeOH 95/5 v/v). White waxy solid 770 mg, yield 98%.

*3,4-bis((3-(dimethylamino)propyl)(methyl)amino)cyclobut-3-ene-1,2-dione (**11**)*.[12b] R_1R_2NH = R_3R_4NH = N,N,N'-trimethyl-1,3-propanediamine (1.03 mL, 6.82 mmol) neat. The mixture was stirred for 15 h at room temperature. The residue was purified by CC (neutral Al_2O_3). White waxy solid 826 mg, yield 90%. mp 43–45°C. ^{1}H NMR ($CDCl_3$) δ 3.71 (t, J = 7.5 Hz, 4H), 3.17 (s, 6H), 2.30 (t, J = 7.2 Hz, 4H), 2.22 (s, 12H), 1.81 (m, 4H). ^{13}C NMR ($CDCl_3$) δ 184.2, 169.4, 56.6, 51.4, 45.7, 39.8, 26.47; ESI(+)-HRMS *m/z* (%) calcd for $C_{16}H_{31}N_4O_2$ $[M+H]^+$ 311.2447; found 311.2448.

*3-((3-(dimethylamino)propyl)(methyl)amino)-4-(phenylamino)cyclobut-3-ene-1,2-dione (**12**)*. To a solution of the squaramic acid ethyl ester **5a** (500 mg, 2.3 mmol) in EtOH (15 mL) was added neat N,N,N'-trimethyl-1,3-propanediamine (390 µL, 2.53 mmol). The mixture was stirred at 80°C for 48 h. After solvent removal at vacuo, the residue was purified by CC (silica gel) to afford **12** as a white solid 507 mg, yield 77%. mp 132–134 ºC. ^{1}H NMR (CD_2Cl_2) δ 10.64 (br s, 1H), 7.31 (t, J = 7.2 Hz, 2H), 7.2 (d, J = 7.5 Hz, 2H), 7.01 (t, J = 7.2 Hz, 1H), 3.5 (br t, J = 5.1 Hz, 2H), 3.37 (s, 3H), 2.45 (br t, J = 5.1 Hz, 2H), 2.3 (s, 6H), 1.83 (br m, 2H). ^{13}C NMR (CD_2Cl_2) δ 186.0, 182.1, 171.3, 164.5, 139.9, 129.3, 122.8, 118.9, 54.3, 48.1, 44.8, 35.9, 22.9. ESI(+)-HRMS *m/z* (%) calcd for $C_{16}H_{22}N_3O_2$ $[M+H]^+$ 288.1712; found 288.1709.

*3-((2,6-diisopropylphenyl)amino)-4-((3-(dimethylamino)propyl)(methyl)amino) cyclobut-3-ene-1,2-dione (**13**)*

Diethyl squarate (500 mg, 2.94 mmol) and 2,6-diisopropylaniline (1,21 mL, 5.9 mmol) were heated at 100 °C under stirring for 48 h. The dilution of the resulting oil with CH_2Cl_2 (10 mL) induced the precipitation of the double diisopropylaniline squaramide (140 mg). This solid was washed with CH_2Cl_2 (3 × 5 mL). The combined CH_2Cl_2 extracts were purified by CC (silica gel) to give an oily product which was treated with pentane to induce the precipitation of the ethyl ester **13a** 406 mg, yield 46%. mp 155-157 ºC. ^{1}H NMR ($CDCl_3$) δ 7.36 (t, J = 7.8 Hz, 1H), 7.18(d, J = 7.5 Hz, 2H), 6.95 (br s, 1H), 4.57(q, J = 6.9 Hz, 2H), 3.07 (m, 2H), 1.23 (t, J = 7.2 Hz, 3H), 1.19 (d, J = 6.9 Hz, 12H). ^{13}C NMR ($CDCl_3$) δ 189.5, 184.1, 179.2, 172.5, 146.4, 131.2, 129.4, 123.7, 69.7, 28.8, 23.7, 15.8. ESI(+)-HRMS *m/z* (%) calcd for $C_{36}H_{46}N_2O_6Na$ $[2M+Na]^+$ 625.3254; found 625.3251. Anal Calcd for $C_{18}H_{23}NO_3$ C, 71.73; H, 7.69; N, 4.65; found C, 71.63; H, 7.41; N, 4.88.

A solution of **13a** (500 mg, 1.66 mmol) and N,N,N'-trimethyl-1,3-propanediamine (304 µL, 1.99 mmol) in EtOH (15 mL) was heated under stirring at 50 °C for 24 h. After solvent removal, the residue was purified by CC (neutral Al_2O_3). White solid 356 mg, yield 58%. mp 110–112°C. ^{1}H NMR ($CDCl_3$) δ 9.66 (br s, 1H), 7.29 (t, J = 7.8 Hz, 1H), 7.14 (d, J = 7.8 Hz, 2H), 3.38 (br m, 5H), 3.14 (m, 2H), 2.38 (br m, 2H), 2.14 (s, 6H), 1.78 (br s, 2H), 1.18 (d, J = 6.9 Hz). ^{13}C NMR ($CDCl_3$, 50ºC) δ 185.1, 182.8, 169.2, 168.3, 146.7, 133.6, 129.1, 124.1, 55.7, 50.2, 45.5, 37.3, 25.7, 23.9, 23.7. ESI(+)-HRMS *m/z* (%) calcd for $C_{22}H_{34}N_3O_2$ $[M+H]^+$ 372.2651. found 372.2660. Anal Calcd for $C_{22}H_{33}N_3O_2$ C, 71.12; H, 8.95; N, 11.31; found C, 71.06; H, 8.59; N, 11.23.

*3-(diisopropylamino)-4-((3-(dimethylamino)propyl)(methyl)amino)cyclobut-3-ene-1,2-dione (**14**)*. To a solution of the squaramic acid ethyl ester **6a** (500 mg, 2.22 mmol) in EtOH (15 mL) was added N,N,N'-trimethyl-1,3-propanediamine (490 µL, 2.89 mmol). The mixture was stirred at 80°C for 48 h. After solvent removal at vacuo, the residue was purified partially by CC (SiO_2; CH_2Cl_2/MeOH, 90/10 v/v) to afford an oily product. The mixture was digested four times at room temperature in a mixture of CH_2Cl_2 (1 mL) and *n*-pentane (20 mL). After decantation, to discard the insoluble material, the organic extracts were pooled and concentrated at vacuo to afford **14** as a thick oil 350 mg, yield 53%. ^{1}H NMR ($CDCl_3$) δ 3.81 (m, 2H), 3.57 (t, J = 7.2 Hz, 2H), 3.11 (s, 3H), 2.27 (t, J = 7.2 Hz, 2H), 2.19 (s, 6H), 1.79 (m, 2H), 1.38 (d, J = 6.9 Hz, 12H). ^{13}C NMR ($CDCl_3$) δ 184.7, 183.6, 170.6, 170.2, 56.6, 51.2, 50.3, 45.6, 38.9, 26.1, 22.6. ESI(+)-HRMS *m/z* (%) calcd for $C_{16}H_{30}N_3O_2$ $[M+H]^+$ 296.2333; found 296.2332.

NMR experiments

A 5 mm NMR tube was loaded with ca. 3 mg of compound **10** and dissolved in 0.70 mL of D_2O. Then, 50 µL of a solution of NaOD (40 wt. % in D_2O) was added to give a ca.

0.9 M solution of NaOD. NMR spectra were measured at room temperature immediately before and after the addition of base. The effect of base addition was as follows: ^{1}H NMR (400 MHz, 298 K, D_2O, ppm) δ 1.05→0.87 (t, 3H), 1.50→1.30 (m, 2H), 1.74→1.49 (m, 2H), 2.23→1.79 (m, 2H), 3.00→2.16 (s, 6H), 3.28→2.32 (t, 2H), 3.39→3.25 (s, 3H), 3.78→3.59 (t, 2H), 3.87→3.65 (br s→t).

The sample with compound **10** was kept at 37 ºC for 300 min (to obtain the maximum amount of partial hydrolysis intermediate according to kinetic data) and 7 days (to achieve complete hydrolysis). The NMR spectra are compared with those of -squaramides **1** and **4** and the complete hydrolysis products A+B (free amines).

^{1}H NMR (400 MHz, 298 K, D_2O, ppm) δ 0.80 (t, **1**+A), 1.26 (m, **1**+A), 1.51 (m, **1**+A), 1.73 (m, **4**), 2.07 (s, B), 2.09 (s, **4**), 2.18 (s, B), 2.23 (m, **4**+B), 2.40 (t, B), 2.49 (t, **1**+A), 3.16 (s, **4**), 3.45 (t, **1**), 3.54 (t, **4**).

Preliminary kinetic studies: Samples of **1**, **4** and **10**, were kept at 37 ºC in 10 mL vials sealed with screw caps with silicone/PTFE septa. After 0, 40, 105 and 189 days, 2 mL aliquots were taken out and measured in a Cary 50 UV-Vis spectrophotometer.

Kinetic experiments: The experiments were carried out on a Cary 50 Bio UV-Vis spectrophotometer at 37.0 ± 0.1 °C (and 45, 50, 55 and 60 ºC for Eyring plots) in water. Solutions of the squaramic acid or squaramide (10^{-5} M; $\varepsilon_{max} \sim 20 - 30 \cdot 10^3$ M^{-1} cm^{-1}) were mixed with a solution of the hydroxide in a range of concentration sufficient (0.01 – 1.00 M) to ensure pseudo-first order conditions. The ionic strength was kept constant through the experiments using the required amounts of the corresponding chloride salts (0.15 and 1 M). The spectral changes in the 200-900 nm range were analysed with the program SPECFIT-32.[19]

Computational details: DFT calculations were performed using Gaussian 09 (Revision D.01).[33] The M06-2X functional,[34] in combination with the cc-pVTZ basis set[35] was used throughout. The effects of the solvent (H_2O, $\varepsilon = 78.3553$) were taken into account self-consistently through the polarizable continuum model (PCM) method.[36] All stationary points were fully characterized via analytical frequency calculations at the same level of theory as either minimum (all positive eigenvalues) or transition states (one negative eigenvalue). This method also provided the corrections required to obtain the solution free energies reported in the text (298.15 K, 1 atm). IRC calculations and subsequent geometry optimisations were used to confirm the minima linked by each transition state. Regarding the calculations in the presence of an explicit H_2O molecule, in some cases the rearrangement of the tetrahedral intermediates resulting from the hydroxide attack was required before the C□N bond cleavage to take place. Nevertheless, these were found to have a small impact on their stabilities, as they mainly involved changes in the relative position of the solvent molecule. Structures were illustrated using CYLview.[37]

Acknowledgments

Financial support from the Spanish Ministry of Economy and Competitiveness (MINECO) (CTQ2011-27512/BQU and CONSOLIDER-INGENIO 2010 CSD2010-00065, FEDER funds) are gratefully acknowledged. M. X. thanks Govern de les Illes Balears for a predoctoral fellowship, FSE funds).

Supporting Information

^{1}H and ^{13}C NMR spectra of new compounds. UV and 1H NMR spectra of hydrolyzed mixtures. Calculated thermodynamic data, DFT calculated structures and Cartesian coordinates for all DFT-optimised species. This material is available free of charge via the Internet at http://pubs.acs.org.

References and Footnotes

[1] (a) Alemán, J.; Parra, A.; Jiang, H.; K. A. Jørgensen, K. A. *Chem. Eur. J.* **2011**, *17*, 6890-6899. (b) Ian Storer, R.; Aciro, C.; Jones, L. H. *Chem. Soc. Rev.* **2011**, *40*, 2330-2346. (c) Wurm, F. R.; Klok, H. -A. *Chem. Soc. Rev.* **2013**, *42*, 8220-8236. (d) Chauhan, P.; Mahajan, S.; Kaya, U.; Hack, D.; Enders, D. *Adv. Synth. Catal.* **2015**, *357*, 253-281.

[2] (a) Ambrosi, G.; Formica, M.; Fusi, V.; Giorgi, L.; Guerri, A.; Micheloni, M.; Paoli, P.; Pontellini, R.; Rossi, P. *Chem. Eur. J.* **2007**, *13*, 702-712. (b) Soberats, B.; Martínez, L.; Sanna, E.; Sampedro, A.; Rotger, C.; Costa, A. *Chem. Eur. J.* **2012**, *18*, 7533-7542. (d) Qin, L.; Hartley, L. A.; Turner, P.; Elmes, R. B. P.; Jolliffe, K. A. *Chem. Sci.* **2016**, *7*, 4563-4572.

[3] (a) Yang, W.; Yang, Y.; Du, D.-M. *Org. Lett.* **2013**, *15*,1190 – 1193. (b) Nair, D. K.; Menna-Barreto, R. F. S.; da Silva Jr, E. N.; Mobin, S. M.; Namboothiri, I. N. N. *Chem. Commun.* **2014**, *50*, 6973-6976. (c) Zhou, E.; Liu, B.; Dong, C. *Tetrahedron Asymmetry* **2014**, *25*, 181-186. (d) Bera, K.; Namboothiri, I. N. N. *J. Org. Chem.* **2015**, *80*, 1402-1413. (e) Sun, Q. -S.; Zhu, H.; Chen, Y. -J.; Yang, X. -D.; Sun, X. -W.; Lin, G. -Q. *Angew. Chem. Int. Ed.* **2015**, *54*, 13253-13257.

[4] (a) Han, X.; Zhou, H. -B.; Dong, C. *Chem. Rec.* **2016**, *16*, 897-906. (b) Held, F. E.; Tsogoeva, S. B. *Catal. Sci. Tech.* **2016**, *6*, 645-667.

[5] (a) Hutchings, M. G.; Ferguson, I.; Allen, S.; Zyss, J.; Ledoux, I. *J. Chem. Res.* **1998**, 244-245. (b) Ohsedo, Y.; Miyamoto, M.; Tanaka, A.; Watanabe, H. *New. J. Chem.* **2013**, *37*, 2874-2880. (c) Saez Talens, V.; Englebienne, P.; Trinh, T. T.; M. Noteborn, W. E.; Voets, I. K.; Kieltyka, R. E. *Angew. Chem. Int. Ed.* **2015**, *54*, 10502-10506.

[6] (a) Busschaert, N.; Kirby, I. L.; Young, S.; Coles, S. J.; Horton, P. N.; Light, M. E.; Gale, P. A. *Angew. Chem. Int. Ed.* **2012**, *51*, 4426-4430. (b) Busschaert, N.; Elmes, R. B. P.; Czech, D. D.; Wu, X.; Kirby, I. L.; Peck, E. M.; Hendzel, K. D.; Shaw, S. K.; Chan, B.; Smith, B. D.; Jolliffe, K. A.; Gale, P. A. *Chem. Sci.* **2014**, *5*, 3617-3626. (c) Deng, L. -Q.; Lu, Y. -M.; Zhou, C. -Q.; Chen, J. -X.; Wang, B.; Chen, W. -H. *Bioorg. Med. Chem. Lett.* **2014**, *24*, 2859-2862. (d) Wu, X.; Busschaert, N.; Wells, N. J.; Jiang, Y. -B.; Gale, P. A. *J. Am. Chem. Soc.* **2015**, *137*, 1476-1484.

[7] (a) Tomàs, S.; Prohens, R.; Deslongchamps, G.; Ballester, P.; Costa, A. *Angew. Chem. Int. Ed.* **1999**, *38*, 2208-2211. (b) Rostami, A.; Wei, C. J.; Guérin, G.; Taylor, M. S. *Angew. Chem. Int. Ed.* **2011**, *50*, 2059-2062. (c) Elmes, R. B. P.; Turner, P.; Jolliffe, K. A. *Org. Lett.* **2013**, *15*, 5638-5641. (d) Manesiotis, P.; Riley, A.; Bollen, B. *J. Mater. Chem. C* **2014**, *2*, 8990-8995.

[8] (a) Rudd, S. E.; Roselt, P.; Cullinane, C.; Hicks, R. J.; Donnelly, P. S. *Chem. Commun.* **2016**, *52*, 11889-11892. (b) Sampedro, A.; Villalonga-Planells, R.; Vega, M.; Ramis, G.; Fernández de Mattos, S.; Villalonga, P.; Costa, A.; Rotger, C. *Bioconjugate Chem.* **2014**, *25*, 1537-1546.

[9] (a) Grabosch, C.; Hartmann, M.; Schmidt-Lassen, J.; Lindhorst, T. K. *ChemBioChem* **2011**, *12*, 1066-1074. (b) Schieber, C.; Bestetti, A.; Lim, J. P.; Ryan, A. D.; Nguyen, T. -L.; Eldridge, R.; White, A. R.; Gleeson, P. A.; Donnelly, P. S.; Williams, S. J.; Mulvaney, P. *Angew. Chem. Int. Ed.* **2012**, *51*, 10523-10527. (c)

Vaillant, O.; Cheikh, K. E.; Warther, D.; Brevet, D.; Maynadier, M.; Bouffard, E.; Salgues, F.; Jeanjean, A.; Puche, P.; Mazerolles, C.; Maillard, P.; Mongin, O.; Blanchard-Desce, M.; Raehm, L.; Rébillard, X.; Durand, J. -O.; Gary-Bobo, M.; Morère, A.; Garcia, M. *Angew. Chem. Int. Ed.* **2015**, *54*, 5952-5956. (d) Palitzsch, B.; Gaidzik, N.; Stergiou, N.; Stahn, S.; Hartmann, S.; Gerlitzki, B.; Teusch, N.; Flemming, P.; Schmitt, E.; Kunz, H. *Angew. Chem. Int. Ed.* **2016**, *55*, 2894-2898.

[10] (a) Kinney, W. A.; Abou-Gharbia, M.; Garrison, D. T.; Schmid, J.; Kowal, D: M.; Bramlett, D. R.; Miller, T. L.; Tasse, R. P.; Zaleska, M. M.; Moyer, J. A. *J. Med. Chem.* **1998**, *41*, 236-246. (b) Sato, K.; Seio, K.; Sekine, M. *J. Am. Chem. Soc.* **2002**, *124*, 12715-12724. (c) Lee, C. -W.; Cao, H.; Ichiyama, K.; Rana, T. M. *Bioorg. Med. Chem. Lett.* **2005**, *15*, 4243-4246. (d) Seio, K.; Miyashita, T.; Sato, K.; Sekine, M. *Eur. J. Org. Chem.* **2005**, 5163-5170.

[11] (a) Villalonga, P.; Fernández de Mattos, S.; Ramis, G.; Obrador-Hevia, A.; Sampedro, Á.; Rotger, C.; Costa, A. *ChemMedChem* **2012**, *7*, 1472-1480. (b) Fernandez-Moreira, V.; Alegre-Requena, J. V.; Herrera, R. P.; Marzo, I.; Gimeno, M. C. *RSC Advances* **2016**, *6*, 14171-14177. (c) Quintana, M.; Alegre-Requena, J. V.; Marques-Lopez, E.; Herrera, R. P.; Triola, G. *MedChemComm* **2016**, *7*, 550-561.

[12] (a) Kumar, S. P.; C. Gloria, P. M.; Goncalves, L. M.; Gut, J.; Rosenthal, P. J.; Moreira, R.; Santos, M. M. M. *MedChemComm* **2012**, *3*, 489-493. (b) Olmo, F.; Rotger, C.; Ramírez-Macías, I.; Martínez, L.; Marín, C.; Carreras, L.; Urbanová, K.; Vega, M.; Chaves-Lemaur, G.; Sampedro, Á.; Rosales, M. J.; Sánchez-Moreno, M.; Costa, A. *J. Med. Chem.* **2014**, *57*, 987-999. (c) Ribeiro, C. J. A.; Espadinha, M.; Machado, M.; Gut, J.; Gonçalves, L. M.; Rosenthal, P. J.; Prudêncio, M.; Moreira, R.; Santos, M. M. M. *Bioorg. Med. Chem.* **2016**, *24*, 1786-1792.

[13] Rotger, C.; Soberats, B.; Quiñonero, D.; Frontera, A.; Ballester, P.; Benet-Buchholz, J.; Deyà, P. M.; Costa, A. *Eur. J. Org. Chem.* **2008**, 1864-1868.

[14] Rotger, C.; Piña, M. N.; Frontera, A.; Martorell, G.; Ballester, P.; Deyà, P. M.; Costa, A. *J. Org. Chem.* **2004**, *69*, 2302-2308.

[15] Quiñonero, D.; Garau, C.; Frontera, A.; Ballester, P.; Costa, A.; Deyà, P. M. *Chem. Eur. J.* **2002**, *8*, 433-438.

[16] Prohens, R.; Tomàs, S.; Morey, J.; Deyà, P. M.; Ballester, P.; Costa, A. *Tetrahedron. Lett.* **1998***, 39*, 1063-1066.

[17] Tomàs, S.; Prohens, P.; Vega, M.; Rotger, M. C.; Deyà, P. M.; Ballester, P.; Costa, A. *J. Org. Chem.* **1996**, *61*, 9394-9401.

[18] (a) Cohen, S.; Cohen, S. G. *J. Am. Chem. Soc.* **1966**, *88*, 1533-1536. (b) Wurm, F.; Steinbach, T.; Klok, H. -A. *Chem. Commun.* **2013**, *49*, 7815-7817. (c) Tietze, L. F.; Schröder, C.; Gabius, S.; Brinck, U.; Goerlach-Graw, A.; Gabius, H.-J. J. *Bioconjugate Chem.* **1991**, *2*, 148-153.

[19] Binstead, R.A.; Jung, B.; Zuberbühler, A. D. *SPECFIT-32*, Spectrum Software Associates: Chappel Hill, 2000.

[20] Laudien, R.; Mitzner, R. J. *Chem. Soc., Perkin Trans. 2*, **2001,** 2226-2229.

[21] (a) Bruylants, A.; Kezdy, F. *Record Chem. Progr.* **1960**, *21*, 213. (b) Kezdy, F.; Bruylants, A. *Bull. Soc. Chim. Belges* **1960,** *69*, 602-615.

[22] Biechler, S. S.; Taft, R. W. *J. Am. Chem. Soc.* **1957**, *79*, 4927-4935.

[23] Mabey, W.; Mill, T. *J. Phys. Chem. Ref. Data* **1978**, *7*, 383-415.

[24] (a) Cox, J. R.; Ramsay, O. B. *Chem. Rev.* **1964**, *64*, 317-352. (b) Williams, N. H.; Wyman, P. *Chem. Commun.* **2001**, 1268-1269.

[25] Talbot, R. J. E. The Hydrolysis of Carboxylic Acid Derivatives. In *Ester Formation and Hydrolysis and Related Reactions, Comprehensive Chemical Kinetics*, Bamford, C. H.; Tipper, C. F. H., Elsevier, Amsterdam, **1972**; *Vol. 10*, pp. 209-287.

[26] O'Connor, C. Q. *Rev. Chem. Soc.* **1970**, *24*, 553-564.

[27] See, for instance: (a) Mujika, J. I.; Mercero, J. M.; Lopez, X. *J. Am. Chem. Soc.* **2005**, *127*, 4445-4453. (b) Xiong, Y.; Zhan, C. -G. *J. Phys. Chem. A* **2006**, *110*, 12644-12652. (c) Cheshmedzhieva, D.; Ilieva, S.; Hadjieva, B.; Galabov, B. *J. Phys. Org. Chem.* **2009**, *22*, 619-631, and references therein.

[28] (a) Lu, T.; Wheeler, S. E. *Chem. Eur. J.* **2013,** *19*, 15141-15147. (b) Kótai, B.; Kardos, G.; Hamza, A.; Farkas, V.; Pápai, I.; Soós, T. *Chem. Eur. J.* **2014**, *20*, 5631-5639.

[29] Note that once the tetrahedral intermediate is generated, it can undergo conformational isomerizations before evolving into products. See ref. 27f.

[30] It is worth noting that intrinsic reaction coordinate (IRC) calculations at **TS_2(5)** followed by structure optimisation also lead to the H-bonded squarate dianion and phenylamine compounds.

[31] Phenylamine has a pK_b ca. 6 units larger than *n*-butylamine. See: M. Silberberg in *Principles of General Chemistry, Third Edition*, McGraw-Hill Higher Education, **2012**.

[32] López, C.; Vega, M.; Sanna, E.; Rotger, C.; Costa, A. *RSC. Advances* **2013**, *3*, 7249-7253.

[33] Frisch, J.; Trucks, G. W.; Schlegel, H. B.; Scuseria, G. E.; Robb, M. A.; Cheeseman, J. R.; Scalmani, G.; Barone, V.; Mennucci, B.; Petersson, G. A.; Nakatsuji, H.; Caricato, M.; Li, X.; Hratchian, H. P.; Izmaylov, A. F.; Bloino, J.; Zheng, G.; Sonnenberg, J. L.; Hada, M.; Ehara, M.; Toyota, K.; Fukuda, R.; Hasegawa, J.; Ishida,

M.; Nakajima, T.; Honda, Y.; Kitao, O.; Nakai, H.; Vreven, T.; Montgomery, Jr., J. A.; Peralta, J. E.; Ogliaro, F.; Bearpark, M.; Heyd, J. J.; Brothers, E.; Kudin, K. N.; Staroverov, V. N.; Kobayashi, R.; Normand, J.; Raghavachari, K.; Rendell, A.; Burant, J. C.; Iyengar, S. S.; Tomasi, J.; Cossi, M.; Rega, N.; Millam, J. M.; Klene, M.; Knox, J. E.; Cross, J. B.; Bakken, V.; Adamo, C.; Jaramillo, J.; Gomperts, R.; Stratmann, R. E.; Yazyev, O.; Austin, A. J.; Cammi, R.; Pomelli, C.; Ochterski, J. W.; Martin, R. L.; Morokuma, K.; Zakrzewski, V. G.; Voth, G. A.; Salvador, P.; Dannenberg, J. J.; Dapprich, S.; Daniels, A. D.; Farkas, Ö.; Foresman, J. B.; Ortiz, J. V.; Cioslowski, J. and Fox, D. J. Gaussian, Inc., Wallingford CT, **2009**.

[34] Zhao, Y.; Truhlar, D. G. *Theor. Chem. Acc.* **2008**, *120*, 215-241.

[35] Woon, D. E.; Dunning, T. H. *J. Chem. Phys.* **1995**, *103*, 4572-4585.

[36] (a) Cossi, M.; Scalmani, G.; Rega, N.; Barone, V. *J. Chem. Phys.* **2002**, *117*, 43-54. (b) Tomasi, J.; Mennucci, B.; Cammi, R. *Chem. Rev.* **2005**, *105*, 2999-3093.

[37] Legault, C. *CYLview v1.0b*, Université de Sherbrooke, Canada, **2009**.

[38] Niewiadomski, S.; Beebeejaun, Z.; Denton, H.; Smith, T. K.; Morris, R. J.; Wagner, G. K. *Org. Biomol. Chem.* **2010***, 8,* 3488-99.

[39] C. Jin, M. Zhang, C. Deng, Y. Guan, J. Gong, D. Zhu, Y. Pan, J. Jiang, L. Wang, *Tetrahedron Lett.* **2013***, 54*, 796-801.

[40] Ehrhardt, H.; Hünig, S.; Pütter, H. *Chem. Ber.* **1977***, 110,* 2506-2523.